European Polymer Journal 190 (2023) 111999

Contents lists available at ScienceDirect

European Polymer Journal

journal homepage: www.elsevier.com/locate/europolj

The microstructure of polyphosphoesters controls polymer hydrolysis kinetics from minutes to years

Timo Rheinberger [a], Mareike Deuker [b], Frederik R. Wurm [a]

[a] Sustainable Polymer Chemistry (SPC), Department of Molecules and Materials, MESA+ Institute for Nanotechnology, Faculty of Science and Technology, University of Twente, P.O. Box 217, 7500 AE Enschede, Netherlands
[b] Max-Planck-Institut für Polymerforschung, Ackermannweg 10, 55128 Mainz, Germany

ARTICLE INFO

Keywords:
Polyphosphoester
Degradation
Hydrolysis
Ring-opening polymerization
Phosphonate

ABSTRACT

The stability and degradation rates of polymers in aqueous media are critical factors for their biomedical applications, as they must remain intact for a specific period of time before degrading or degrading on-demand to prevent potential accumulation and harmful effects. Polyphosphoesters (PPEs) are highly compatible with biological systems, and the ester bonds in the backbone allow for hydrolytic degradation. In this study, we have demonstrated that the degradation rate of various PPEs can be precisely controlled by minor modifications to the side-chain and the binding pattern around the phosphorous center in the polymer backbone. We synthesized a systematic library of water-soluble PPEs using ring-opening polymerization, resulting in polyphosphates and in-chain or side-chain polyphosphonates. Specifically, we investigated the degradation rates of side-chain polyphosphonates with different side-chain structures (methyl, ethyl, allyl, iso- or *n*-propyl) at pH = 8 and pH = 11. Our results indicate that the degradation mechanism is influenced by the type and size of the side-chain, as well as the pH. At pH = 11, hydrophilicity is a key factor, while at pH = 8, electron density on the phosphorus is crucial, leading to a random chain scission or a backbiting mechanism. We also observed that changing the binding pattern of the phosphorus or incorporating additional "breaking points" allowed us to tune the half-life times of the polymer from less than a day to several years. This study highlights the versatile stability of water-soluble PPEs, making them a promising option for various applications that require different hydrolysis rates, such as tissue regrowth.

1. Introduction

Polymers have become an indispensable part of our everyday life. Specifically, water-soluble polymers play an important role in healthcare, cosmetics, medicine or food applications and are produced on a million ton scale per year, the market size in 2021 was USD 30.5 billion [1] and USD 4.3 billion[2] alone for poly(ethylene glycol) (PEG).[3] However, most water-soluble polymers used today are not biodegradable or degrade on either very long or very short time scales. While starch-based systems biodegrade effectively, synthetic water soluble polymers, like polyvinylpyrrolidone, poly(acrylic acid) (PAA) and several polyoxazolines are resistant to biodegradation,[4,5] while PEG and poly(vinyl alcohol) (PVA) biodegrade slowly.[6,7] Such polymers are used in various formulations and applications, either as homopolymers or in copolymers of, for example, PEG-based surfactants, stabilizers, thickeners or surface coatings.[8] Other polymers like PVA or polyacrylates, in particular PAA, are used for similar applications also as copolymers with PEG.[9] However, as already shown in the pioneering work of Suzuki in the 1970 s, the degradability for high molar mass PAA, PVA, and also PEG is very low. Enzymatic degradation becomes suitable for low molecular PEG and also PVA is slowly degrading – however, no precise control over the degradation kinetics of such water-soluble polymers is possible.[10].

Ongoing research is investigating (bio)degradable alternatives: one widely used strategy to enhance degradability of synthetic polymers is the introduction of labile moieties, so-called "breaking points", e.g. hydrolysis-labile ester or anhydride bonds.[11] They enable a fragmentation of the polymer chain into lower molar mass oligomers, which shall then be further biodegraded by enzymes and microorganisms. [12,13] However, this strategy has not been commercialized so far, due to the increased material costs compared with common polymers and not all resulting oligomers are biodegradable either.

Conversely, natural polymers are biodegradable, but often ill-defined and compared to synthetic polymers obtained with controlled

E-mail address: f.r.wurm@utwente.nl (F.R. Wurm).

https://doi.org/10.1016/j.eurpolymj.2023.111999
Received 12 January 2023; Received in revised form 8 March 2023; Accepted 13 March 2023
Available online 18 March 2023

techniques, and as a result they show lower performance when it comes to applications. Although the material properties can be adjusted by chemical modification of the natural polymer, these modifications often lead to a significant reduction with respect to their biodegradability. [14,15] Biopolymers need certain enzymes or microorganisms under specific conditions to be able to degrade the polymers, with chemical modification of polysaccharides, relatively stable materials are obtained, e.g. hydroxy ethyl starch (HES), which had been used in blood substitutes for years.[12].

One class of polymers that does degrade by hydrolysis in aqueous media is the so-called class of polyphosphoesters (PPEs).[16] Hydrophobic, low molar mass PPEs are used as halogen-free flame retardants, while also water-soluble PPEs with adjustable molar mass and chemical structure are researched today for biomedical applications.[17,18] Well-defined PPEs are prepared by anionic ring-opening polymerization (AROP) from phospholane-monomers (cyclic, five-membered phosphoesters) and are often discussed as a promising but degradable alternatives to PEG and other water-soluble polymers.[19] PPEs are a broad class of polymers, which exhibit remarkable difference in their hydrolytic stabilities if only the binding pattern of the central phosphorus is altered (Scheme 1): for polyphosphates ($PO(OR)_3$) it was shown that the hydrolysis follows mainly a backbiting mechanism as known from polylactide (PLA) by Bauer *et al.*[20] *(*poly(ethyl ethylene phosphate) (PEEP) was studied). Wolf et al. showed first indications that the side-chains in polyphosphonates ($PO(OR)_2R'$ with the R'-group located in the side-chain of the polymer) influences the hydrolysis rates from hours to weeks, whereas in-chain polyphosphonates ($PO(OR)_2R'$ with the R'-group located in the main-chain of the polymer) exhibited much longer hydrolysis half-life times.[21,22] While all these polymers remained water-soluble, the hydrolysis times could be altered in a systematic way. However, so far, no such systematic and long-term study of a library of water soluble PPEs has been investigated.

Here, we provide a systematic study on the hydrolysis of different water-soluble polyphosphoesters, including polyphosphates, and in- and side-chain polyphosphonates. We studied the hydrolysis via a combination of ^{1}H and ^{31}P NMR spectroscopy over a period of several years where necessary. The data underlines the previous separate findings that the binding pattern around the central phosphorus atom and the nature of the side-chains influences the degradation kinetics and mechanism, which ultimately allows one to control the half-life times of PPEs in aqueous conditions.[23] We believe such findings will help the design of novel biodegradable devices for biomedical and other applications.

2. Results and discussion

2.1. Synthesis

We synthesized a library of well-defined and water-soluble PPEs with variable binding pattern around the phosphorus and different side chains via organocatalytic, anionic ring-opening polymerization (AROP, Fig. 1).[24,25] All polymers were prepared to have a similar degree of polymerization of ca. 100 repeating units. The syntheses of the monomers and the initial reports on their polymerization can be found in the literature.[21,22,26–29] To enlarge our library, we also prepared a so far not reported polyphosphonate, carrying an *n*-propyl side chain. Since

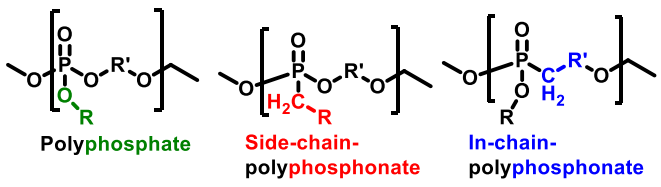

Scheme 1. General structure of polyphosphates, side- and in-chain polyphosphonates.

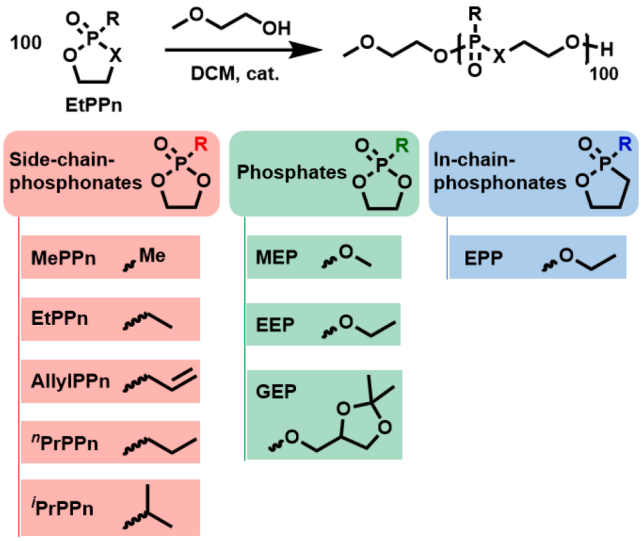

Fig. 1. Synthesis scheme for the anionic ring-opening polymerisation of cyclic phospholanes and resulting PPE-library used in this study.

the monomer for the *n*-propyl side-chain phosphonate cannot be achieved by the common synthesis methods (isomerization to the isopropyl derivative occurs during the synthesis as outlined by Wolf et al. [21,22]), we used the allyl-derivative polyphosphonate P(AllylPPn) (4) [27] and hydrogenated the double bonds to obtain 5. The hydrogenation was conducted using Pd on carbon and hydrogen and was quantitative with no changes of the molar mass distribution during the hydrogenation. All synthesized polymers and their characteristics are summarized in Table 1, the experimental details are reported in Experimental Section.

To investigate the correlation between the microstructure of each polymer and its effect on hydrolytic stability, we monitored the degradation of each polymer using ^{31}P and ^{1}H NMR spectroscopy at two distinct pH values (pH = 8 and pH = 11) within the NMR tube. To obtain viable 1H NMR spectra, the degradation was carried out in a buffered H_2O/D_2O mixture of 9:1. It should be noted that due to insufficient suppression of the water signal, not all signals in ^{1}H NMR were quantitatively monitored during the degradation. We will first discuss each polymer class individually, followed by an overview of the hydrolysis stabilities of the entire PPE library.

Hydrolysis of side-chain polyphosphonates.

Since the side-chain polyphosphonates do not have a hydrolysable side-chain, only the polymer backbone can be hydrolyzed (Fig. 1, red series). We expected a backbiting mechanism to occur at moderate pH-values similar to the reported polyphosphates.[20] When an end-capped side-chain polyphosphonate was hydrolyzed at pH = 11, only very slow degradation was detected (Fig. 2), while the same polymer with a free OH-end group hydrolyzed in only a few hours as determined from ^{31}P NMR (Fig. 2). For the end-capping, the terminal OH-group was blocked by termination of the polymerization reaction with ethyl isocyanate as reported earlier for P(EEP).[20] The slow hydrolysis of the end-capped PPE could be caused presumably by the much slower random chain scission.

A detailed investigation on the hydrolysis mechanism of polymers 1–6 was carried out using a combination of ^{31}P NMR and ^{1}H NMR spectroscopy. (Fig. 3a and b display the degradation of P(MePPn) (1) as an exemplary case) The ^{1}H NMR spectra displayed broad resonances of the polymer backbone protons at 4.2 ppm for the diesters and the protons of the side-chain at approximately 1.6 ppm. During the hydrolysis, additional sharp resonances at 3.6, 3.8, and 1.1 ppm were observed, indicating the degradation product, a phosphonic acid monoester. The integrals of these resonances were monitored over time, and the hydrolysis kinetics of each polymer were plotted (Fig. 3c,d). The hydrolysis

Table 1
Overview over reaction conditions of the polymerizations and polymer characteristics.

#	Polymer	Cat.	CoCat.	temp. / °C	Reaction time / h	P_n [a]	M_n [a] / kg•mol^{-1}	$Đ$ [b]
1	P(MePPn)	DBU	–	0	4	104	12.7	1.20
2	P(EtPPn)	DBU	–	0	16	96	13.0	1.15
3	P(EtPPn)capt	DBU	–	0	16	60	8.2	1.14
4	P(AllylPPn)	DBU	–	0	16	134	19.9	1.07
5	P(^{n}PrPPn)	hydrogenation of P(AllyPPn) with Pd/C				110	16.6	1.13
6	P(^{i}PrPPn)	TBD	–	0	0.5	98	14.7	1.13
7	P(EPP)	DBU	TrisUrea	−10	48	85	12.8	1.17
8	P(MEP)	DBU	TU	0	1.5	92	12.7	1.21
9	P(EEP)	DBU	TU	0	1.5	97	14.8	1.06
10	P(EEP$_{95}$-*co*-GEP$_5$)	DBU	TU	0	1.5	85	13.3	1.33
10d	P(EEP$_{95}$-*co*-^{d}GEP$_5$)	deprotected P(EEP$_{95}$-*co*-GEP$_5$)				85	13.2	n.d.
11	P(EEP$_{90}$-*co*-GEP$_{10}$)	DBU	TU	0	1.5	89	14.3	1.39
11d	P(EEP$_{90}$-*co*-^{d}GEP$_{10}$)	deprotected P(EEP$_{90}$-*co*-GEP$_{10}$)				89	14.2	n.d.

a) determined by ^{1}H NMR spectroscopy, b) determined by size exclusion chromatography (SEC) in DMF vs. PEG standards (elugrams shown in SI Fig. S1); DBU = 1,8-Diazabicyclo[5.4.0]undec-7-ene, TBD = 1,5,7–Triazabicyclo[4.4.0]dec-5-en, TU = 1(3,5-bis(trifluoromethyl)phenyl)-3-cyclohexyl thiourea, TrisUrea = 1,1′,1″–(nitrilotris(ethane-2,1-diyl))tris(3-(3,5-bis(trifluoromethyl)phenyl)urea), *n.d.* = not determined.

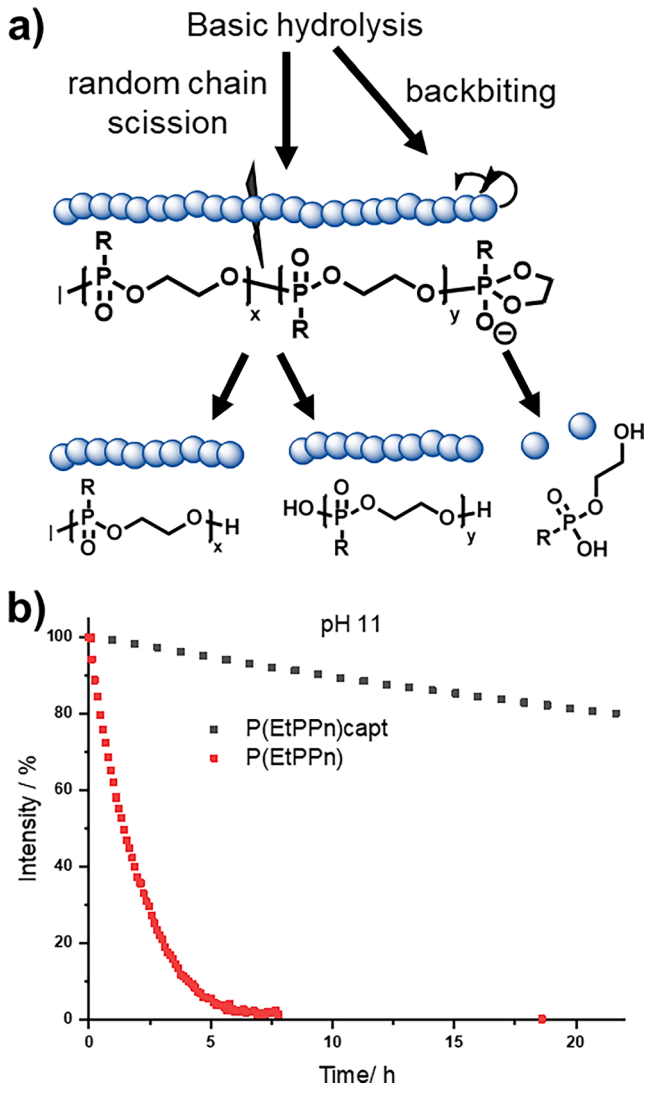

Fig. 2. Backbiting vs random chain scission a) schematic illustration of the competing processes, b) the end-capped polymer is degrading slowly since no backbiting from the end cannot occur.

followed a first-order reaction, which indicated the dominance of the backbiting mechanism. The half-life times were calculated from the data, and the SEC traces supported the backbiting degradation as a random chain scission would lead to additional distributions (Fig. 3e). The first-order decay of the polymer signal in the ^{31}P NMR spectra gave a linear relation with the natural logarithm of the polymer signal, which was utilized to determine a rate constant (k_1) for the backbiting degradation reaction (Fig. 3f). The rate constant and half-life times are listed in Table 2. Notably, no further hydrolysis of the phosphonic acid monoester was observed under the given conditions. Supplementary information contains further details on hydrolysis kinetics.

To analyze the hydrolysis rates of polymers 2–6, we followed the same approach as described for P(MePPn) at pH = 11. The degradation kinetics for each polyphosphonate were determined by plotting half-lives ($t_{1/2}$) and rate constants (k_1), which are shown in Fig. S2-6. The comparison of the hydrolysis rates for all side-chain polyphosphonates is presented in Fig. 4, and the values for $t_{1/2}$ and the rate constant are summarized in Table 2. At pH = 11 (Fig. 4a), the half-life increased with the length of the side chain, indicating that the hydrophilicity of the polymer plays a significant role in its lability. The hydrophilicity of the polymers was also determined by reverse-phase HPLC, where an increase in elution volume reflects a decrease in the polymer hydrophilicity. In addition, logP values were calculated for all polymers using a previously reported method.[30] A clear correlation between hydrophilicity and degradation rates was observed. The correlation is apparent when the hydrolysis rate constants at pH = 11, the logP values, and the elution volume from the rp-HPLC are plotted (Fig. 4c). Conversely, at pH = 8, a different trend was observed for the degradation rates (Fig. 4b). The allyl-functionalized polyphosphonate in the side chain exhibited the fastest hydrolysis kinetics at pH = 8, followed by methyl, ethyl, and *iso*-propyl. The *iso*-propyl-functionalized polyphosphonate exhibited significantly higher stability under these conditions. We hypothesize that this trend is due to the different abilities depending on the nature of the side-chain to form a five-membered ring, which is the intermediate during the backbiting degradation. The alcohol group at the chain end attacks the phosphorus in a nucleophilic fashion, which is determined by the electron density at the phosphorus center. The allyl group has a slight electron-withdrawing effect, making cyclization easier, followed by the *n*-alkyl substituents. For the *iso*-propyl group, the increased electron-donating effect and steric hindrance seem to be responsible for the drastically reduced degradation rate at pH = 8.

Hydrolysis of polyphosphates.

When considering the hydrolysis of polyphosphates (PO(OR)$_3$) with a hydrolysable side-chain (Fig. 1 green series), a competition between main-chain and side-chain cleavage is anticipated (Scheme 2 and Fig. 4a). Bauer *et al.* studied the hydrolysis of P(EEP) and showed that the main-chain cleavage was favored over side-chain hydrolysis. DFT calculations underlined that the main-chain cleavage was energetically favored vs. the side-chain cleavage.[20] As for the polyphosphonates, a

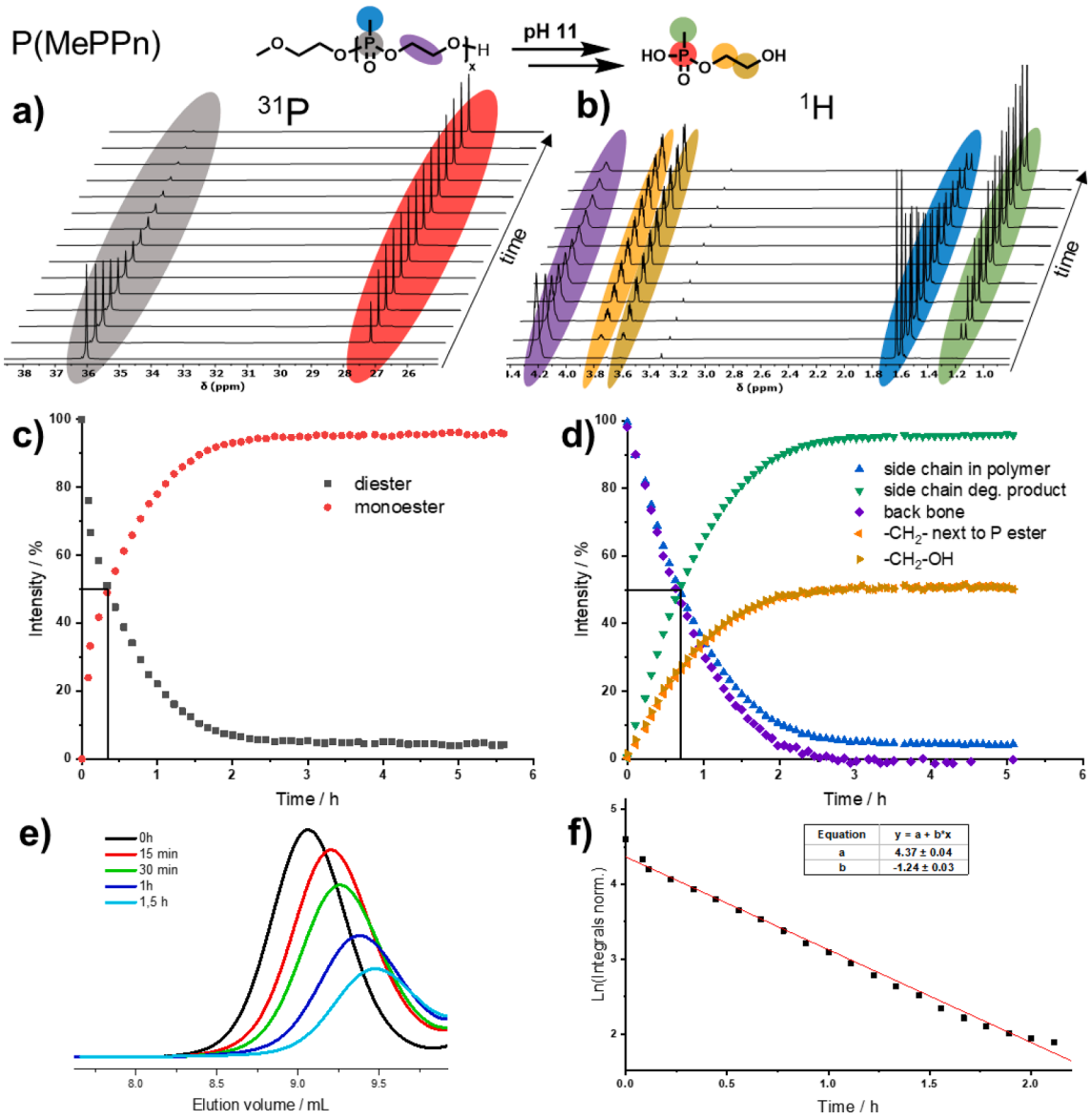

Fig. 3. Real-time NMR and SEC data for the hydrolysis of P(MePPn) at pH = 11 shows first-order degradation kinetics. a) Overlay of the $^{31}P\{^{1}H\}$ NMR spectra (500 MHz, 298 K, in H_2O:D_2O 9:1) measured over 5.5 h (interval between each spectrum 13 min); b) Overlay of the ^{1}H NMR spectra (500 MHz, 298 K, in H_2O:D_2O 9:1) measured over 5 h (interval between each spectrum 13 min); c) normalised integrals of the polymer signal and the degradation product determined from ^{31}P NMR spectra, plotted vs. time show exponential decay of the polymer signal; d) exponential decay of the polymer followed by the ^{1}H NMR spectra by the resonances of both backbone and side chain; e) size exclusion chromatograms showing a continuous shift to higher elution times during the degradation, indicating the backbiting mechanism; f) First-order degradation kinetics plot and reaction constant k.

single main degradation product was detected, ethyl ethylene phosphate in this case, i.e. a phosphoric acid diester (so, only one bond had been cleaved under the investigated conditions and time). Here, we expanded the degradation studies and followed the degradation of P(MEP) (8) and P(EEP) (9) over a period of almost four years at pH = 8 and 11 and included copolymers 10 and 11 with additional breaking points placed in the main chain (see below).

To monitor the degradation of the polymers, a combination of ^{31}P and ^{1}H NMR spectroscopy was used at pH = 11. Fig. 5b and c show the integrals of the resonances of labeled atoms in Fig. 5a over time. The hydrolysis of the polymer was quantified by monitoring the change in the integral of the phosphorus atom triester (at −1.25 ppm) hydrolyzed into diester (at 0.8 ppm) and the methyl protons in the side chain (at 1.28 ppm in the polymer, at 1.16 ppm in the diester degradation product and at 1.08 ppm in the released ethanol). The integral of the diester increased during main-chain cleavage and followed the same progress as the methyl protons of the ethyl ester in the beginning (up to 200 days). Additional degradation products were observed in the ^{31}P NMR spectra due to hydrolysis of the diester and transesterification reactions.

Transesterification seems to be the most likely reaction, as the signal of free ethanol did not increase after 100 days of hydrolysis, while the amount of further degradation products increased, and the ethyl ester signal increased as well. At pH = 8, further degradation/transesterification occurred, but the overall degradation was slower. The rate constant for the backbiting reaction (k_1) within the first day of hydrolysis was calculated from the natural logarithm of the polymer signal vs. time (Scheme 2, Fig. 5e blue fit). Side-chain hydrolysis also occurred (main-:side-chain ca. 20:1 over 24 h), resulting in more polymer chains carrying a negatively charged phosphodiester group, which likely prevents backbiting from occurring.

This accumulation of negatively charged chains in combination with backbiting degradation results in a nonlinear correlation of the

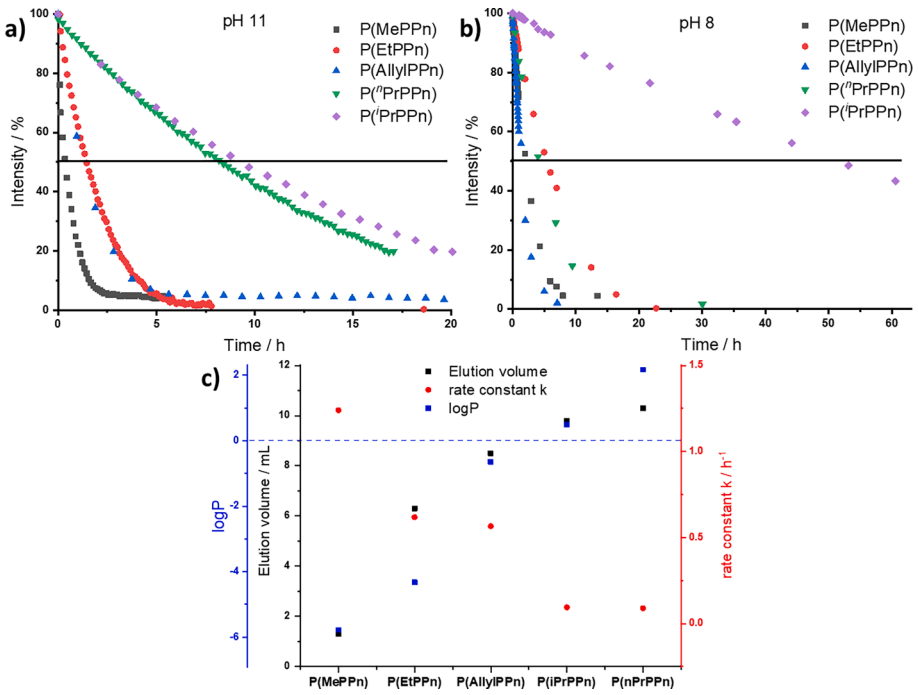

Fig. 4. All side-chain polyphosphonates show first order degradation kinetics with different half-life times a) polymer hydrolysis determined by ^{31}P NMR at pH = 11 and b) at pH = 8, c) the rate constants determined at pH = 11 show a reciprocal relation to the hydrophilicity, plotted as logP value and retention time from rp-HPLC.

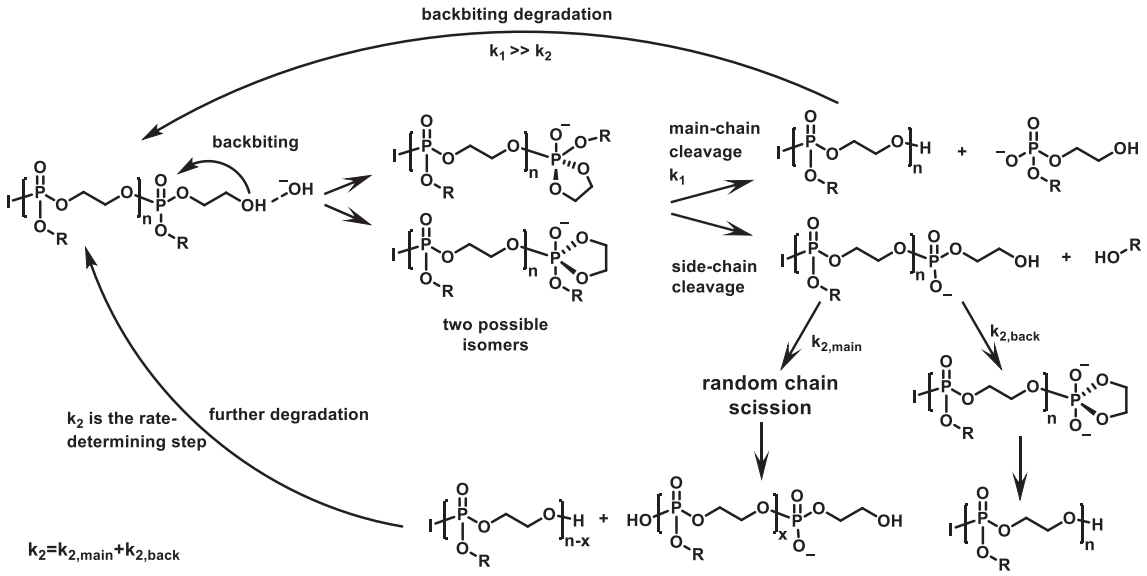

Scheme 2. Degradation mechanism of polyphosphates suggested by Bauer et al., based on DFT calculations the main-chain cleavage is energetically preferred[20] with a rate constant k_1, due to the side-chain cleavage, over time all chains carry a charged diester at the polymer chain end, which slows down the degradation, and the rate-determining step for further degradation (k_2) of the shielded polymers becomes a combination of random chain scission ($k_{2,main}$) and second back biting ($k_{2,back}$).

degradation rate (Fig. 4e intermediate times). After 200 days, a linear decrease of the phosphotriesters was observed, which presumably shows the combined kinetics of random main-chain scission (with a rate constant $k_{2,main}$) and the backbiting of a negatively charged phosphate end group (with a rate constant $k_{2,back}$, Scheme 2). These secondary degradation steps are expected to be the rate-determining steps at this stage of the degradation, and the obtained rate constant k_2 is the sum of these two pathways listed in Table 2 (Scheme 2, Fig. 4e).

In contrast, at pH = 8, a linear trend was not observed in the beginning of the hydrolysis kinetics, indicating a more complex degradation pathway of combined backbiting and random chain scission (SI Fig. S10). The second rate constant k_2 was observed, and all values are listed in Table 2.

The situation changed, when the hydrolysis of the more hydrophilic P(MEP) was analyzed (SI Fig. S9). In contrast to P(EEP), at pH = 11, for P(MEP) no linear trend was observed in the beginning of the logarithmic plot (SI Fig. S9c). The initial degradation rates were higher than those for P(EEP), but the preferred degradation product was not the expected diester after the main-chain cleavage (Fig. S9a). As the methyl ester side-chains are more prone to hydrolysis, more side reactions can occur, leading to an increased polymer half-life time compared to P(EEP).

At pH = 8, P(MEP) was hydrolyzed ca. 20 times faster than P(EEP) at

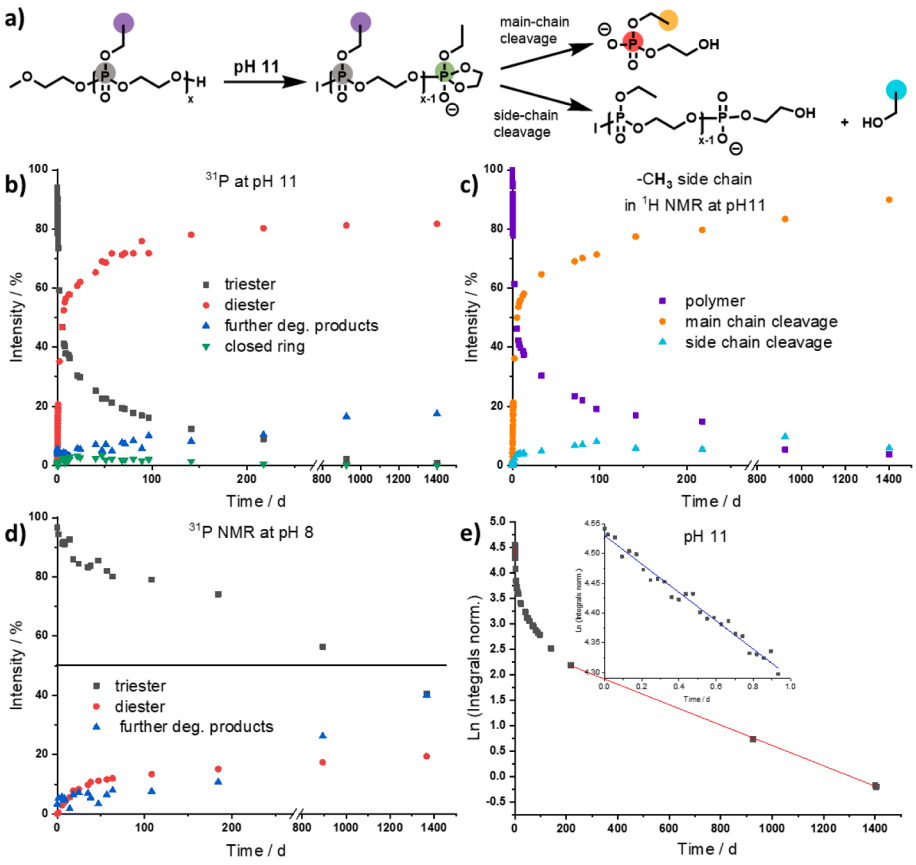

Fig. 5. During the polyphosphate degradation several processes are competing: a) during the back biting process the main-chain or side-chain can be cleaved; b) the decay of the polymer signal and the formation of the diester as degradation product from the main-chain cleavage followed by ^{31}P NMR and plotted vs. time, b) ^{1}H NMR spectra allow following competing reactions plotted vs. time; d) the degradation kinetics at pH = 8; e) the polymer degradation from **a** (logarithmic plot) shows two different linear regions, which were fitted and give two hydrolysis rate constants.

Table 2
Summary of the half-life-times and rate constants for hydrolysis of all polymers at pH 8 and pH 11.

#	Polymer	$t_{1/2}$ pH 11	$t_{1/2}$ pH 8	k_1 / h^{-1} pH 11	k_1 / h^{-1} pH 8	k_2 / h^{-1} pH 11	k_2 / h^{-1} pH 8
1	P(MePPn)	0.3 h	2.0 d	1.240	0.015	–	–
2	P(EtPPn)	1.5 h	5.3 d	0.618	0.007	–	–
4	P(AllylPPn)	1.2 h	1.4 d	0.566	0.023	–	–
5	P(^{n}PrPPn)	8.2 h	4.3 d	$8.9*10^{-2}$	$8.2*10^{-3}$	–	–
6	P(^{i}PrPPn)	9.0 h	49 d	$9.4*10^{-2}$	$5.2*10^{-4}$	–	–
7	P(EPP)	98 d	3836 d[a]	–	–	$6.1*10^{-5}$	$6.0*10^{-6}$
8	P(MEP)	6.9 d	45 d	–	–	$9.0*10^{-5}$	$1.3*10^{-4}$
9	P(EEP)	3.7 d	1064 d	$9.9*10^{-3}$	–	$8.3*10^{-5}$	$2.1*10^{-5}$
10	P(EEP_{95}-*co*-GEP_5)	7.7 d	n.D.	$7.7*10^{-3}$	–	–	–
10d	P(EEP_{95}-*co*-$^{d}GEP_5$)	1.2 d	18 d	$2.3*10^{-2}$	–	–	–
11	P(EEP_{90}-*co*-GEP_{10})	6.9 d	n.D.	$1.0*10^{-2}$	–	–	–
11d	P(EEP_{90}-*co*-$^{d}GEP_{10}$)	0.9 d	4.8 d	$2.8*10^{-2}$	–	–	–

All values are calculated from the intensity change of the polymer signal in the ^{31}P NMR spectra, k_1 is the rate constant of the backbiting degradation, k_2 is the rate constant of random chain scission and second back biting. a) The data after 4 years were fitted like all other degradation curves and the half life time is an approximation from the fit.

pH = 8. From the ^{31}P NMR spectra, almost only additional degradation products were visible (Fig. S9b), indicating a less controlled degradation. This makes P(MEP) especially appealing for hydrogels with a fast release kinetics as only a few ester cleavage steps break the crosslinks, as reported previously.[31].

To accelerate the degradation of the P(EEP), we introduced breaking points in the polymer chain. GEP, a monomer carrying an acetal-protected glycerol side-chain was copolymerized with EEP as outline in Scheme 3.[32] After mild acidic hydrolysis of the acetal groups, pendant OH-groups are released, which should lead to accelerated backbone cleavage by intramolecular transesterification (Scheme 3). This concept was already introduced by Kosrev *et al.* who showed very fast hydrolysis of homopolymers of GEP,[33] and by our group as the so-called "RNA-inspired" degradation in other copolymers.[34,35] Here, we used GEP only as a comonomer and statistically copolymerized it with EEP in a 1:9 and 1:19 ratio. The protected copolymers, i.e. P(EEP-*co*-GEP) (**10** and **11**) exhibited the same degradation rates as the P(EEP)-homopolymer both at pH = 8 and 11 (Fig. S11a, b and S13a, b). However, after release of the OH-groups, the degradation rates increased significantly. At pH = 11, a ca. 3 times faster hydrolysis was observed (Fig. S11c, d). The rate constant was determined to be $2.3*10^{-2}h^{-1}$ and $2.8*10^{-2}h^{-1}$ (Fig S12, Table 2). At pH = 8, the additional OH-groups have an even higher effect on the overall polymer stability: while the homopolymer P(EEP) exhibited a half-life time of ca. 1000 days under these condition, the copolymer with 5% comonomer (P(EEP_{95}-*co*-$^{d}GEP_5$) (10d) showed a half-life time of 18 days and P(EEP_{90}-*co*-$^{d}GEP_{10}$) of only

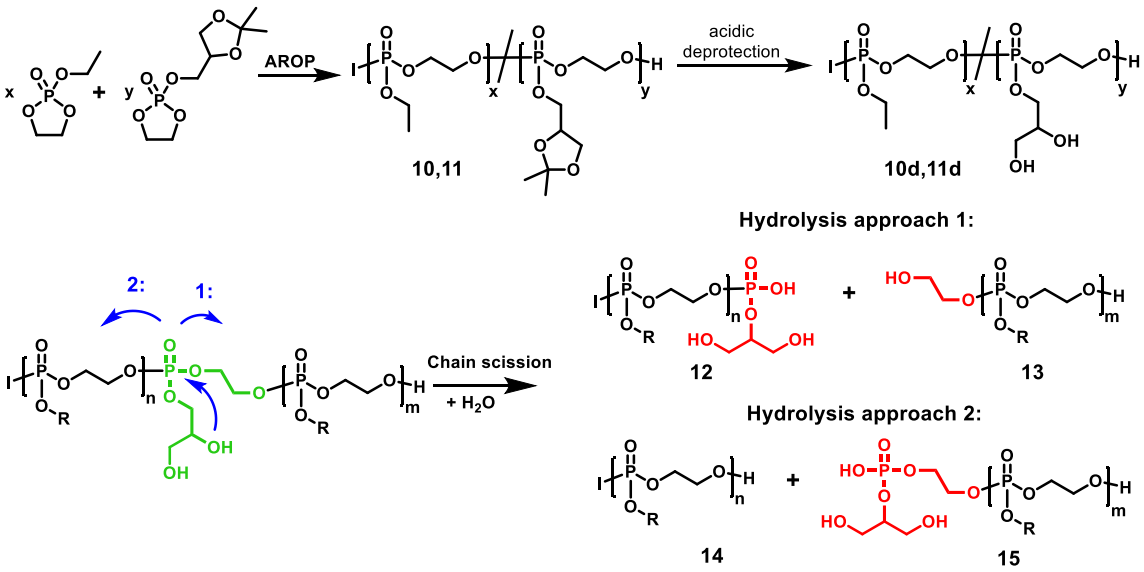

Scheme 3. Synthesis scheme of P(EEP-*co*-GEP) **10** and **11** copolymers and the deprotected P(EEP-*co*-^{d}GEP) **10d** and **11d**. Two possible ways of hydrolysis in the first step leading to different intermediates.

5 days (Fig. S13c, d). This 50 and 200 times, faster degradation by intramolecular transesterification was achieved by introducing only 5 and 10 % of the GEP comonomer, underlining the power of the RNA-inspired polymer degradation. Scheme 3 shows the possible degradation pathways for the deprotected GEP-containing copolymers following the intramolecular attack of the pendant OH-groups. As reported by Kosrev et al., no 6-membered intermediate was detected during the hydrolysis,[33] and we assume that for the P(EEP-*co*-GEP)-copolymers also only the energetically favored, 5-membered intermediate is responsible for the main chain scission. The different resulting fragments (12–15, Scheme 3) undergo further hydrolysis, which in total led to an accelerated degradation compared to the PEEP-homopolymer.

Hydrolysis of in-chain polyphosphonates.

One report has utilized phostones to create in-chain polyphosphonates with hydrolysis-stable P-C-bonds in the main chain (Fig. 1, blue series). However, only the ethyl-derivative (EPP) has been reported as water-soluble to date.[22] Bauer *et al.* initially reported an extremely low hydrolysis rate for in-chain polyphosphonates, which have two competing hydrolysable bonds: one in the main chain and one in the side-chain.

Hydrolysis of the polymer was quantified by measuring the change in the integral of the phosphonic acid diester in the polymer (at 34.7 ppm), which hydrolyzes into the monoester (at 28.1 ppm) and further degradation products (at 27 and 36 ppm) (SI Fig. S7a). The competition between main- and side-chain cleavage can be quantified by measuring the integral of the methyl protons in the side chain (at 1.24 ppm in the polymer, at 1.14 ppm in the diester degradation product and at 1.08 ppm in the released ethanol) (SI Fig. S7b). At pH = 11, P(EPP) (9) exhibited a higher amount of side-chain cleavage compared to P(EEP) (main-:side-chain 3:1 average during the measurement). This also explains the overall slower degradation, as the resulting negatively charged chains only slowly further hydrolyze (SI Fig. S7c,d). The rate constant k_2 was calculated to be $6.1*10^{-5}h^{-1}$, which is in the same order of magnitude as P(EEP) (Table 2).

At pH 8, less than 30% of P(EPP) was degraded after almost 4 years, and the half-life time was obtained from the fit curve in the same way as for the other polymers, with the fit curve being plotted beyond the data points (SI Fig. S8c). A rate constant k_2 was determined to be 10 times slower compared to pH = 11 (6.0*10–6 h^{-1}). Therefore, the overall degradation is really slow, making it the most stable polymer among the tested PPEs.

3. Summary and conclusion

We systematically analyzed the hydrolysis mechanism of a library of several polyphosphoesters, including polyphosphates, in- and side-chain polyphosphonates, and copolymers with hydrolysis-accelerating breaking points. We followed the hydrolysis of the polymers at pH = 8 and pH = 11 by ^{1}H and ^{31}P NMR over a period of >three years. We determined the half-life times and rate constants for the backbiting (k_1) and further hydrolysis (k_2) for quantifying the degradation kinetics.

We found that the side-chain polyphosphonates followed the simplest hydrolysis pathway, as only the polymer backbone could degrade. We demonstrated that the degradation kinetics were controlled by the nature of the side-chain. At pH = 11, the degradation rate was determined by the hydrophilicity of the side-chain, while at pH = 8, the degradation rate was dependent on the electron donating or withdrawing effects of the side-chain to the central phosphorus atom. We observed that the ability to form the five-membered intermediate for the backbiting varied with the nature of the side-chain, and the branched isopropyl side chain led to a slowed-down hydrolysis compared to the respective *n*-propyl derivative due to further steric effects.

For polyphosphates, the degradation process was more complex since the side-chain hydrolysis competed with main-chain cleavage by backbiting. If the side-chain was hydrolyzed, a negatively charged phosphodiester resulted, which significantly slowed down further degradation of the polymer. After >200 days, all remaining oligomers/polymers were capped by a negatively charged diester, and the main driving force of the degradation became a combination of random chain scission and second back biting, which was much slower than the preferred backbiting degradation. We found that RNA-inspired degradation was efficient in increasing the hydrolysis rates of polyphosphates by installing a few breaking points for intramolecular transesterification into the polymer backbone, which provided a further handle to control polymer stability.

When we installed a stable P-C bond in the main-chain of a polyphosphonate, we observed that a high number of side-chain cleavage resulted in the inhibition of further polymer degradation, making these polymers the most stable of the currently known polyphosphoester family.

In conclusion, PPEs cover a broad range of hydrolysis rates, depending on the chemistry around the central phosphorus and the chemical nature of their side-chains. We presented a rough overview of the high diversity of degradation kinetics observed in the PPEs we

studied, where half-life times ranged from less than one hour to several years. Our systematic long-term study on the hydrolysis of PPEs sets the basis for the future development of (bio)degradable PPE-based materials. Fig. 6 provides an overview of the diverse degradation kinetics we observed in the PPEs studied.

4. Experimental

4.1. Materials and methods

Materials.

All solvents were purchased in HPLC grade or dry (purity > 99.8 %) and chemicals were purchased in the highest grade (purity > 98 %) from *Sigma Aldrich, Acros Organics, Fluka VWR chemicals* or *Fisher Scientific* and used as received unless otherwise described. 1,8-Diazabicyclo [5.4.0]undec-7-ene (DBU) was distilled from calcium hydride and stored over molecular sieves (3 and 4 Å) under a nitrogen atmosphere. 2-(Benzyloxy)ethanol was purchased from *ABCR*, distilled from calcium hydride, and stored over molecular sieves (4 Å) under a nitrogen atmosphere. Ethylene glycol was purchased dry and stored over molecular sieves (4 Å) under nitrogen atmosphere. 1,5,7-Triazabicyclo[4.4.0]dec-5-en (TBD) was freeze-dried bevor use.

2-methyl-2-oxo-1,3,2-dioxaphospholane (MePPn) was synthesised according to the two-step procedure described by Steinbach *et al.*[26] 2-ethly-2-oxo-1,3,2-dioxaphospholane (EtPPn), 2-isopropyl-2-oxo-1,3,2-dioxaphospholane (^{i}PrPPn) and 2-allyl-2-oxo-1,3,2-dioxaphospholane (AllylPPn) were synthesised according to the two-step procedure described by Wolf *et al.*[21,27] 2–ethoxy-1,2-oxaphospholane 2-oxide (EPP) was synthesised according to the procedure described by Bauer *et al.*[22] 2-methoxy-2-oxo-1,3,2-dioxaphospholane (MEP) and 2-ethoxy-2-oxo-1,3,2-dioxaphospholane (EEP) was synthesised according to the procedure described by Steinbach *et al.*[28] 2-(2,2-dimethyl-1,3-dioxolan-4-yl-methoxy)-2-oxo-1,3,2-dioxaphospholane (GEP) was synthesised according to the procedure described by Song *et al.*[29] The monomers were stored at −25 °C under a nitrogen atmosphere.

Size exclusion chromatography (SEC).

Size exclusion chromatography (SEC) measurements were performed in DMF (containing 1 g·L^{-1} of LiBr) at 60 °C and a flow rate of 1 mL min^{-1} with a *PSS SECcurity* as an integrated instrument, including three *PSS GRAM* column (100/1000/1000 g mol-1) and a refractive index (RI) detector. Calibration was carried out using poly(ethylene glycol) standards supplied by *Polymer Standards Service*. The SEC data were plotted with *OriginPro* 2019b software from *OriginLab* Corporation.

Degradation was monitored by aqueous SEC. Samples were separated over a set of Suprema Lin S columns with a flow rate of 1.0 mL min^{-1} in 100 mM phosphate, 50 mM sodium chloride, pH 6.5. Each sample injection was 50 µL.

Nuclear Magnetic Resonance (NMR) Spectroscopy.

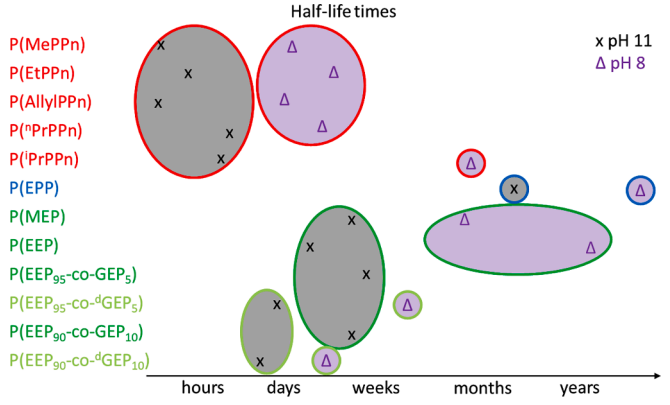

Fig. 6. Graphical summary of the half-life times of PPEs investigated in this study.

The ^{1}H, and ^{31}P NMR spectra were measured on a 300 MHz, 400 MHz, 500 MHz or 700 MHz *Bruker AVANCE III AMX* system or 600 MHz *Bruker AVANCE NEO* system. The temperature was kept at 298.3 K. As deuterated solvent DMSO-d_6, $CDCl_3$ or D_2O were used. For analysis of all measured spectra *MestReNova* 9 from *Mestrelab Research S.L.* was used. The spectra were calibrated against the solvent signal. Degradation studies were recorded on a 300 MHz, 400 MHz or 500 MHz *Bruker AVANCE III AMX* system. All degradation studies were conducted in a buffer containing 10% D_2O.

LogP values were calculated from https://www.molinspiration.com. Polymers were approximated by 12 monomer units with methoxy end-group. Note: For hydrophobic compounds, logP values are > 0 whereas the logP value for hydrophilic substances is less than 0.

Half-life times were determined from the decreasing polymer signal in the ^{31}P NMR spectra, normalised integrals were plotted with *OriginPro* 2019b and fitted with a exponential fit (ExpDec2).

Polymer synthesis.

Representative procedure for the ring-opening polymerization catalyzed with DBU or TBD.

Polymerization was performed according to modified literature protocols.[21,26] The respective monomers were weighed in a flame-dried Schlenk-tube, dissolved in dry benzene and dried by three times lyophilization. The monomer was dissolved in dry dichloromethane to a total concentration of 4 mol L^{-1}. A stock solution of initiator 2-methoxyethanol in dry dichloromethane was prepared with a concentration of 0.2 mol L^{-1} and the calculated amount was added to the monomer solution via Hamilton® syringe. A stock solution of DBU or TBD in dry dichloromethane was prepared with a concentration of 0.2 mol L^{-1}. The monomer solution and the catalyst solution were set to the respective reaction temperature (in general 0 °C).

The polymerization was initiated by the addition of the calculated volume of catalyst solution containing 3.0 equivalents of DBU or TBD in respect to the initiator. Polymerization was terminated by the rapid addition of an excess of formic acid dissolved in dichloromethane with a concentration of 20 mg mL^{-1}. The colorless, amorphous polymers were purified by precipitation into cold diethyl ether and dialyzed against pure water over night and dried at reduced pressure. Yields ranged from 70% to 90%.

5. Representative NMR data of P(MePPn)

^{1}H NMR ($CDCl_3$, ppm): δ = 4.24–4.09 (m, backbone –CH_2-), 3.32 (s, initiator –CH_3-O-), 1.50 (d, $^{2}J_{HP}$ = 18 Hz, P-CH_3).

^{31}P NMR ($CDCl_3$, ppm): δ = 32.34.

6. Representative NMR data of P(EtPPn)

^{1}H NMR ($CDCl_3$, ppm): δ = 4.26–4.10 (m, backbone –CH_2-), 3.32 (s, initiator CH_3-O-), 1.82–1.68 (m, side-chain P-CH_2-), 1.17–1.05 (m, side-chain –CH_3).

^{31}P NMR ($CDCl_3$, ppm): δ = 35.24.

7. Representative NMR data of P(^{i}PrPPn)

^{1}H NMR ($CDCl_3$, ppm): δ = 4.25–4.10 (m, backbone –CH_2-), 3.32 (s, initiator CH_3-O-), 2.03–1.85 (m, side-chain P-CH-), 1.18–1.04 (m, side-chain –CH_3).

^{31}P NMR ($CDCl_3$, ppm): δ = 36.83.

8. Representative NMR data of P(AllylPPn)

^{1}H NMR ($CDCl_3$, ppm): δ = 5.81–5.65 (m, side-chain –C**H** = CH_2), 5.23–5,14 (m, side-chain –CH = C**H$_2$**), 4.26–4.08 (m, backbone –CH_2-), 3.31 (s, initiator CH_3-O-), 2.68–2.58 (dd, side-chain P-CH_2-).

^{31}P NMR ($CDCl_3$, ppm): δ = 28.63.

9. Representative NMR data of P(^{i}PrPPn-*co*-EtPPn)

^{1}H NMR ($CDCl_3$, ppm): δ = 4.29–4.19 (m, backbone –CH_2-), 3.39 (s, initiator CH_3-O-), 2.06–1.99 (m, side-chain P-CH-), 1.85–1.79 (m, side-chain P-CH_2-), 1.23–1.16 (m, side-chain –CH_3).

^{31}P NMR ($CDCl_3$, ppm): δ = 36.84 (P-CH-$(CH_3)_2$), 35.20 (P-CH_2-CH_3).

Synthesis of poly(*n*-propyl-2-oxo-1,3,2dioxaphospholane) P (^{n}PrPPn).

Poly(2-Allyl-2-oxo-1,3,2dioxaphospholane) (200 mg) was dissolved in 10 mL dry ethanol in a glass vessel and the solution was degassed by bubbling argon through the solution for 15 min. 30 mg of 10 wt% Pd/C was added and the glass vessel was charged into a 250 mL ROTH autoclave. Hydrogenation was performed at 70 °C and 50 bar H_2 for 24 h. After completion of the reaction, the reaction mixture was filtered. The product was dried at reduced pressure to yield the polymer as a colorless viscous liquid in quantitative yield.

^{1}H NMR ($CDCl_3$, ppm): δ = 4.25–4.07 (m, backbone –CH_2-), 3,32 (s, initiator CH_3-O-), 1.78–1.53 (m, side-chain P-CH2-CH2-), 0.96 (t, J = 7.5 Hz, –CH_3).

^{31}P NMR ($CDCl_3$, ppm): δ = 33.84.

Representative procedure for the ring-opening polymerization catalyzed with DBU and co-catalyst 1(3,5-bis(trifluoromethyl)phenyl)-3-cyclohexyl thiourea (TU) or 1,1′,1″–(nitrilotris(ethane-2,1-diyl))tris(3-(3,5-bis(trifluoromethyl)phenyl)urea) (TrisUrea).

Polymerization was performed according to a modified literature protocol.[22] The co-catalyst TU or TrisUrea weighed in a flame-dried Schlenk-tube, dissolved in dry benzene and dried by lyophilization. The respective monomers were weighed in a flame-dried Schlenk-tube, dissolved in dry benzene and dried by lyophilization. The monomer was dissolved in dry dichloromethane to a total concentration of 4 mol L^{-1}. A stock solution of initiator 2-methoxyethanol in dry dichloromethane was prepared with a concentration of 0.2 mol L^{-1} and the calculated amount was added to the monomer solution via Hamilton syringe ®. A stock solution of DBU in dry dichloromethane was prepared with a concentration of 0.2 mol L^{-1}. The monomer solution and the catalyst solution were set to the respective reaction temperature (in general 0 °C).

The polymerization was initiated by the addition of the calculated volume of catalyst solution containing 3.0 equivalents of DBU in respect to the initiator. Polymerization was terminated by the rapid addition of an excess of formic acid dissolved in dichloromethane with a concentration of 20 mg mL^{-1}. The colorless, amorphous polymers were purified by precipitation into cold diethyl ether and dialyzed against pure water over night and dried at reduced pressure. Yields ranged from 70% to 96%.

10. Representative NMR data of P(EPP)

^{1}H NMR ($CDCl_3$, ppm): δ = 4.10–3.97 (m, backbone P-CH_2-C**H**$_2$-C**H**$_2$-O/ side-chain P-O-CH_2-), 3.32 (s, initiator CH_3-O), 1.96–1-70 (m, backbone P-C**H**$_2$-), 1.27 (t, J = 7.5 Hz, side-chain –CH_3).

^{31}P NMR ($CDCl_3$, ppm): δ = 31.45.

11. Representative NMR data of P(MEP)

^{1}H NMR ($CDCl_3$, ppm): δ = 4.26–4.19 (m, backbone –CH_2-), 3,77–3,71 (m, side-chain P-O-CH_3), 3.32 (s, initiator CH_3-O-).

^{31}P NMR ($CDCl_3$, ppm): δ = -0.19.

12. Representative NMR data of P(EEP)

^{1}H NMR ($CDCl_3$, ppm): δ = 4.26–4.05 (m, P-O-CH_2-), 3,32 (s, initiator CH_3-O-), 1.29 (t, J = 7.5 Hz, side-chain –CH_3).

^{31}P NMR ($CDCl_3$, ppm): δ = -1.30.

13. Representative NMR data of P(EEP-*co*-GEP)

^{1}H NMR (DMSO-d_6, ppm): δ = 4.26–4.01 (m, backbone –CH_2–, side-chain P-O-CH_2– and side-chain P-O-CH_2-CH-CH_2–), 3,32 (s, initiator CH_3-O-), i1.33 (s, protection group –CH_3), 1.29 (t, J = 7.5 Hz, side-chain –CH_3).

^{31}P NMR ($CDCl_3$, ppm): δ = -1.36.

Deprotection of P(EEP-*co*-GEP) to yield P(EEP-*co*-^{d}GEP).

The deprotection was performed according to a literature protocol.[29] 200 mg of the protected copolymer were dissolved in 30 mL 1,4-Dioxan. 5 mL of 1 M HCl solution were added slowly and afterwards stirred for 3 h. The colorless, amorphous polymers were purified by precipitation in cold diethyl ether and dried in vacuo. The protection group was removed quantitative.

14. Representative NMR data of P(EEP-*co*-^{d}GEP)

^{1}H NMR (DMSO-d_6, ppm): δ = 4.26–4.01 (m, backbone –CH_2–, side-chain P-O-CH_2– and side-chain P-O-CH_2-CH-CH_2–), 3,32 (s, initiator CH_3-O-), 1.26 (t, J = 7.5 Hz, side-chain –CH_3).

^{31}P NMR ($CDCl_3$, ppm): δ = -1.36.

Degradation.

Buffer solution pH = 11.

40 mL buffer solution (pH 11) was prepared by adding 20 mL of 0.4 M $NaHCO_3$-solution with 7.4 mL of 1 M NaOH solution and 8.6 mL H_2O and 4 mL D_2O to achieve a H_2O:D_2O ratio 9:1. The pH of the buffer was determined with a pH electrode.

Buffer solution pH = 8.

Saturated $NaHCO_3$ solution was prepared and added to MilliQ water until pH 8 was reached. 5 mL D_2O were added to 45 mL of this solution to achieve a H_2O:D_2O ratio 9:1. The pH of the buffer was determined with pH electrode.

Data availability

Raw data can be made available upon request from the authors.

CRediT authorship contribution statement

Timo Rheinberger: Data curation, Formal analysis, Investigation, Writing – original draft, Writing – review & editing, Methodology. **Mareike Deuker:** Data curation, Formal analysis, Investigation. **Frederik R. Wurm:** Conceptualization, Formal analysis, Funding acquisition, Supervision, Writing – original draft, Writing – review & editing.

Declaration of Competing Interest

The authors declare that they have no known competing financial interests or personal relationships that could have appeared to influence the work reported in this paper.

Data availability

Data will be made available on request.

Acknowledgments

The authors acknowledge funding by the University of Twente and the German Research Foundation (DFG, WU750/ 6-2).

Appendix A. Supplementary data

Supplementary data to this article can be found online at https://doi.org/10.1016/j.eurpolymj.2023.111999.

References

[1] M. Intelligence, Water Soluble Polymer Market – Growth, Trends, Covid-19 Impact, and Forecasts (2023–2028), Mordor Intelligence (2022).
[2] P.S. intelligence,, Polyethylene Glycol Market Size and Share Analysis by Form, Grade and Application-Forecast to 2030, Prescient & Strategic intelligence (2022).
[3] S. Koltzenburg, M. Maskos, O. Nuyken, Polymere in Lösung, in: S. Koltzenburg, M. Maskos, O. Nuyken (Eds.), Polymere: Synthese, Eigenschaften und Anwendungen, Springer Berlin Heidelberg, Berlin, Heidelberg, 2014, pp. 19-41.
[4] M. Boerman, E. Roozen, G. Franssen, J. Bender, H. Richard, S. Leeuwenburgh, P. Laverman, J. Hest, H. Goor, R. Felix Lanao, Degradation and excretion of poly(2-oxazoline) based hemostatic materials, Materialia 12 (2020), 100763.
[5] I. Gaytán, M. Burelo, H. Loza-Tavera, Current status on the biodegradability of acrylic polymers: microorganisms, enzymes and metabolic pathways involved, Appl Microbiol Biotechnol 105 (3) (2021) 991–1006.
[6] E. Chiellini, A. Corti, S. D'Antone, R. Solaro, Biodegradation of poly (vinyl alcohol) based materials, Prog. Polym. Sci. 28 (6) (2003) 963–1014.
[7] F. Kawai, Biodegradation of Polyethers (Polyethylene Glycol, Polypropylene Glycol, Polytetramethylene glycol, and Others), Biopolymers Online.
[8] J. Herzberger, K. Niederer, H. Pohlit, J. Seiwert, M. Worm, F.R. Wurm, H. Frey, Polymerization of Ethylene Oxide, Propylene Oxide, and Other Alkylene Oxides: Synthesis, Novel Polymer Architectures, and Bioconjugation, Chem. Rev. 116 (4) (2016) 2170–2243.
[9] J. Riemer, T. Russo, The Use of Thickeners in Topically Applied Formulations, Handbook of Formulating Dermal Applications (2016) 29.
[10] J. Suzuki, K. Hukushima, S. Suzuki, Effect of ozone treatment upon biodegradability of water-soluble polymers, Environ. Sci. Tech. 12 (10) (1978) 1180–1183.
[11] M. Worm, D. Leibig, C. Dingels, H. Frey, Cleavable Polyethylene Glycol: 3,4-Epoxy-1-butene as a Comonomer to Establish Degradability at Physiologically Relevant pH, ACS Macro Lett. 5 (12) (2016) 1357–1363.
[12] G. Swift, Environmentally Biodegradable Water-Soluble Polymers, in: G. Scott (Ed.), Degradable Polymers: Principles and Applications, Springer, Netherlands, Dordrecht, 2002, pp. 379–412.
[13] G.W.M. Vandermeulen, A. Boarino, H.-A. Klok, Biodegradation of water-soluble and water-dispersible polymers for agricultural, consumer, and industrial applications—Challenges and opportunities for sustainable materials solutions, J. Polym. Sci. 60 (12) (2022) 1797–1813.
[14] N. Yadav, M. Hakkarainen, Degradable or not? Cellulose acetate as a model for complicated interplay between structure, environment and degradation, Chemosphere 265 (2021), 128731.
[15] T. Haider, C. Völker, J. Kramm, K. Landfester, F.R. Wurm, Plastics of the future? The impact of biodegradable polymers on the environment and on society, Angew. Chem. Int. Ed. doi:10.1002/anie.201805766(ja).
[16] T. Steinbach, F.R. Wurm, Poly(phosphoester)s: A New Platform for Degradable Polymers, Angew Chem Int Ed Engl 54 (21) (2015) 6098–6108.
[17] C. Wachiralarpphaithoon, Y. Iwasaki, K. Akiyoshi, Enzyme-degradable phosphorylcholine porous hydrogels cross-linked with polyphosphoesters for cell matrices, Biomaterials 28 (6) (2007) 984–993.
[18] Z.E. Yilmaz, C. Jérôme, Polyphosphoesters: New Trends in Synthesis and Drug Delivery Applications, Macromol. Biosci. (2016) n/a-n/a.
[19] C. Pelosi, M.R. Tinè, F.R. Wurm, Main-chain water-soluble polyphosphoesters: Multi-functional polymers as degradable PEG-alternatives for biomedical applications, Eur. Polym. J. 141 (2020), 110079.
[20] K.N. Bauer, L. Liu, M. Wagner, D. Andrienko, F.R. Wurm, Mechanistic study on the hydrolytic degradation of polyphosphates, Eur. Polym. J. 108 (2018) 286–294.
[21] T. Wolf, T. Steinbach, F.R. Wurm, A Library of Well-Defined and Water-Soluble Poly(alkyl phosphonate)s with Adjustable Hydrolysis, Macromolecules 48 (12) (2015) 3853–3863.
[22] K.N. Bauer, L. Liu, D. Andrienko, M. Wagner, E.K. Macdonald, M.P. Shaver, F. R. Wurm, Polymerizing Phostones: A Fast Way to In-Chain Poly(phosphonate)s with Adjustable Hydrophilicity, Macromolecules 51 (4) (2018) 1272–1279.
[23] F.R. Wurm, Binding matters: binding patterns control the degradation of phosphorus-containing polymers, Green Mater. 4 (4) (2016) 135–139.
[24] Y. Iwasaki, E. Yamaguchi, Synthesis of Well-Defined Thermoresponsive Polyphosphoester Macroinitiators Using Organocatalysts, Macromolecules 43 (6) (2010) 2664–2666.
[25] B. Clément, B. Grignard, L. Koole, C. Jérôme, P. Lecomte, Metal-Free Strategies for the Synthesis of Functional and Well-Defined Polyphosphoesters, Macromolecules 45 (11) (2012) 4476–4486.
[26] T. Steinbach, S. Ritz, F.R. Wurm, Water-Soluble Poly(phosphonate)s via Living Ring-Opening Polymerization, ACS Macro Lett. 3 (3) (2014) 244–248.
[27] T. Wolf, T. Rheinberger, J. Simon, F.R. Wurm, Reversible Self-Assembly of Degradable Polymersomes with Upper Critical Solution Temperature in Water, J. Am. Chem. Soc. 139 (32) (2017) 11064–11072.
[28] T. Steinbach, R. Schroder, S. Ritz, F.R. Wurm, Microstructure analysis of biocompatible phosphoester copolymers, Polym. Chem. 4 (16) (2013) 4469–4479.
[29] W.-J. Song, J.-Z. Du, N.-J. Liu, S. Dou, J. Cheng, J. Wang, Functionalized Diblock Copolymer of Poly(ε-caprolactone) and Polyphosphoester Bearing Hydroxyl Pendant Groups: Synthesis, Characterization, and Self-Assembly, Macromolecules 41 (19) (2008) 6935–6941.
[30] J. Simon, T. Wolf, K. Klein, K. Landfester, F.R. Wurm, V. Mailänder, Hydrophilicity Regulates the Stealth Properties of Polyphosphoester-Coated Nanocarriers, Angew. Chem. Int. Ed. 57 (19) (2018) 5548–5553.
[31] H.T. Tee, R. Zipp, K. Koynov, W. Tremel, F.R. Wurm, Poly(methyl ethylene phosphate) hydrogels: Degradable and cell-repellent alternatives to PEG-hydrogels, Eur. Polym. J. 141 (2020), 110075.
[32] L.K. Müller, T. Steinbach, F.R. Wurm, Multifunctional poly(phosphoester)s with two orthogonal protective groups, RSC Adv. 5 (53) (2015) 42881–42888.
[33] M.A. Kosarev, D.E. Gavrilov, I.E. Nifant'ev, A.V. Shlyakhtin, A.N. Tavtorkin, V. P. Dyadchenko, V.A. Roznyatovsky, P.V. Ivchenko, Ultrafast hydrolytic degradation of 2,3-dihydroxypropyl functionalized poly(ethylene phosphates), Mendeleev Commun. 29 (5) (2019) 509–511.
[34] T. Rheinberger, J. Wolfs, A. Paneth, H. Gojzewski, P. Paneth, F.R. Wurm, RNA-Inspired and Accelerated Degradation of Polylactide in Seawater, J. Am. Chem. Soc. 143 (40) (2021) 16673–16681.
[35] M. Pokora, T. Rheinberger, F.R. Wurm, A. Paneth, P. Paneth, Environment-friendly transesterification to seawater-degradable polymers expanded: Computational construction guide to breaking points, Chemosphere 308 (2022), 136381.